ELSEVIER

Materials Science and Engineering B99 (2003) 138–142

MATERIALS SCIENCE & ENGINEERING B

www.elsevier.com/locate/mseb

Preparation and properties of $Sr(Bi_{1-x}Nd_x)_8Ti_7O_{27}$ ceramics for wireless technologies

Z.X. Xiong *, C. Fang, J.R. Huang, H. Qiu, M. Lin

Department of Materials Science and Engineering, Xiamen University, Xiamen 361005, China

Received 14 June 2002; received in revised form 20 September 2002; accepted 21 October 2002

Abstract

$Sr(Bi_{1-x}Nd_x)_8Ti_7O_{27}$ ceramics for wireless technologies were prepared by a solid-state reaction route. Raw materials of $SrCO_3$, Bi_2O_3, Nd_2O_3 and TiO_2 were used. The mixture was ball-milled, dried, and hydro-pressed into pellets or formed into green body by gel-casting, which were then sintered at 1180–1300 °C. Sintering process was analyzed by TGA and DSC. Microstructure of ceramic body was observed by SEM. Crystalline phases of the ceramics were identified by X-ray diffraction. Dielectric properties of the samples were also measured, showing dielectric constant $\varepsilon = 80$–110 and $Qf = 120$–2100 GHz at 10 GHz.

Keywords: Microwave ceramics; Dielectric properties; Gel-casting

1. Introduction

With the popularization of wireless communication, it is of key importance to develop excellent microwave ceramics with high dielectric constant ε, low dielectric loss D or high quality factor Q, and suitable temperature coefficient of resonance frequency τ_f [1–4]. Highly dielectric ceramics make it possible to obviously miniaturize microwave components.

However, it can usually be shown that the temperature coefficient of dielectric constant in ceramics is directly proportional to dielectric constant [5–9]. Such coefficient may be adjusted for different compositions. In this paper, preparation and properties of SBNT, i.e., $Sr(Bi_{1-x}Nd_x)_8Ti_7O_{27}$ ceramics with the aurivillius-type structure were reported, which were formed by hydro-pressing and gel-casting techniques [10].

2. Experimental

Raw materials with chemical purity were used, including $SrCO_3$, Nd_2O_3, TiO_2 and Bi_2O_3. Six kinds of compositions of $Sr(Bi_{1-x}Nd_x)_8Ti_7O_{27}$ were weighted and mixed with different values of $x = 0.05$, 0.1, 0.2, 0.3, 0.4 and 0.5, respectively. Such chemicals were ball-milled, dried and then calcined at 950–1000 °C for 2 h. They were ground into fine powders. Then, two different forming techniques were applied. The first route was to let the powder be milled with a binder of polyvinyl alcohol (PVA) solution, spray-dried for granulating, and then hydro-pressed into pellets. The second one was to mix the powder with a few of organic chemicals, such as AM, MBAM, and water, and then filled into a cast by gel-casting. Below 600 °C, most of green bodies were heated firstly at 600 °C h^{-1} and one kind of it was treated at 60 °C h^{-1}. Then all kinds of samples were heated at 330 °C h^{-1} and finally sintered at 1200–1300 °C for 90 min. Electrodes were formed by reducing the silver oxide paste at 800 °C for 0.5 h.

Thermal analysis of the powders was carried out by TGA and DSC (Netzsch, German). Crystalline phases of the sintered bodies were identified by X-ray diffraction (XRD) (Rigaku, Japan). Microstructure of the ceramics was observed with SEM (Leo, German). Hysteresis loops of the samples were obtained by a ferroelectric measurement system (Radiant, USA). Dielectric properties of the ceramics were measured by a HP 4284A Meter, a HP 4291A Material Analyzer, and a microwave measurement system at 10 GHz [11].

* Corresponding author
E-mail address: zxxiong@xmu.edu.cn (Z.X. Xiong).

0921-5107/02/$ - see front matter © 2002 Published by Elsevier Science B.V.
PII: S0921-5107(02)00504-4

3. Results and discussion

3.1. Thermal analysis of the powders

Fig. 1 illustrates the spectra of the granulated powders with TGA and DSC. It can be seen that there was an exo-thermal peak at about 200 °C, which meant the decomposition of PVA binder within the range of temperature. In the range of 700–1200 °C there was an obvious endo-thermal reaction, which corresponded to main stage of the sample compacting and sintering. Meanwhile the sample lost its weight slightly but continually.

3.2. XRD spectra of ceramics

Major phase of $SrBi_8Ti_7O_{27}$ with aurivillius-type structure was identified by using of XRD technique, in addition to minor phase of $Bi_4Ti_3O_{12}$, for the samples with different values of x, here $x = 0.05$, 0.1, 0.2, 0.3, 0.4 and 0.5, respectively. Fig. 2 displayed an example of the XRD spectrum for the ceramic with $x = 0.4$, sintered at 1300 °C for 90 min.

The samples with $x = 0.5$ were treated in different temperatures, $T = 20$, 950, 1260, 1280 and 1300 °C for 90 min, respectively. With the increasing of treatment temperature, the phase of $SrBi_8Ti_7O_{27}$ became more dominant, as shown in Fig. 3 for the ceramics with $x =$ 0.5. The minor phase of $Bi_4Ti_3O_{12}$, meanwhile, decreased and even disappeared.

3.3. SEM images of the samples

Microstructure of green bodies formed by hydro-pressing and gel-casting were displayed in Fig. 4, respectively. It can be seen that more and larger pores appeared for the green body by gel-casting.

Different ways of sintering were then taken for the samples, sintered at 60 °C h^{-1} (upper) and at 600 °C h^{-1} (lower), respectively. In Fig. 5 the cross-section of ceramic, which was formed by hydro-pressing and then sintered at high speed of heating (600 °C h^{-1}), shows a typical microstructure.

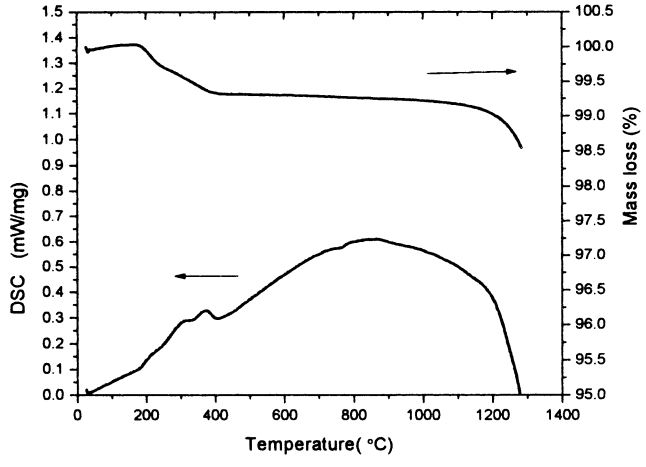

Fig. 1. Spectra of TGA and DSC.

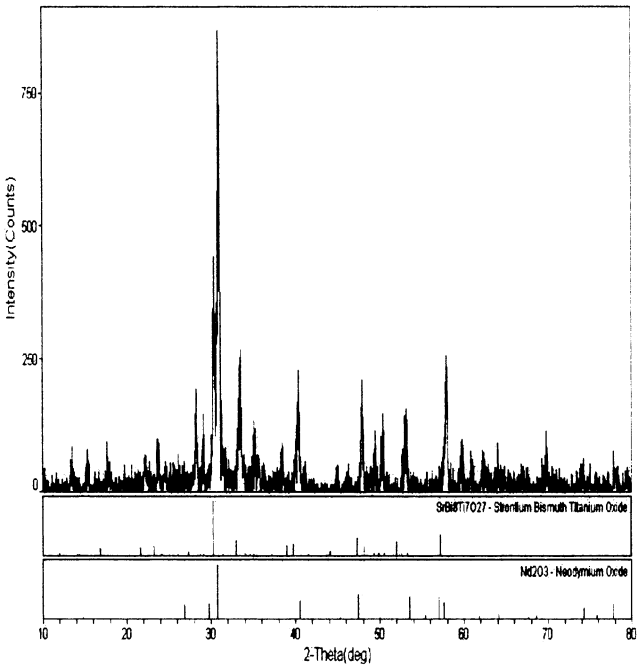

Fig. 2. XRD spectra of the sample with $x = 0.4$, sintered at 1300 °C for 90 min.

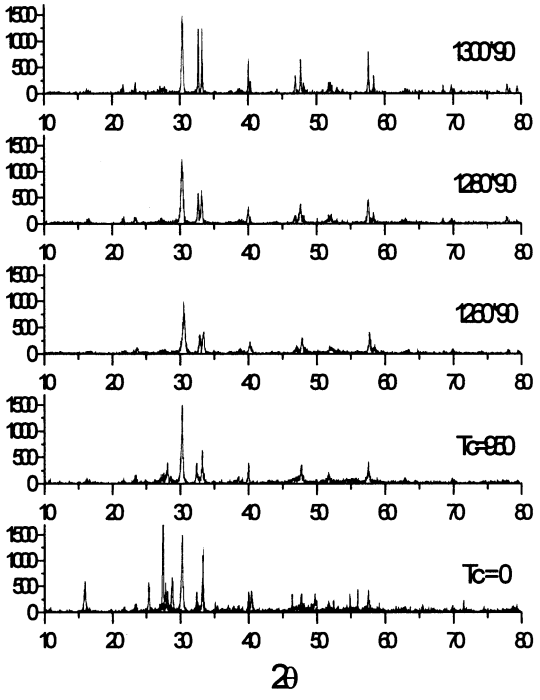

Fig. 3. XRD spectra of the sample with $x = 0.5$, treated at different temperatures.

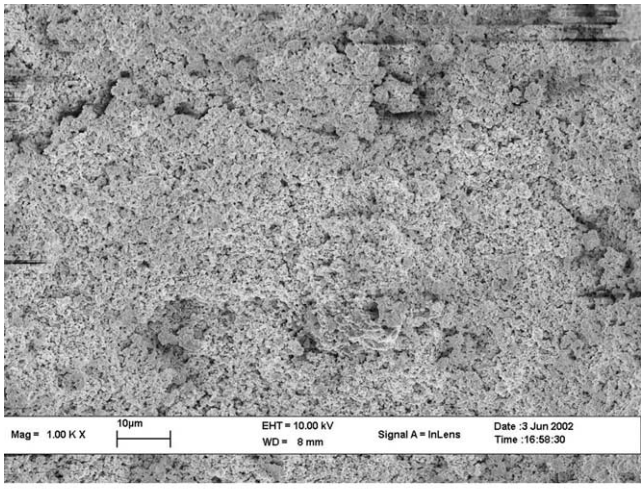

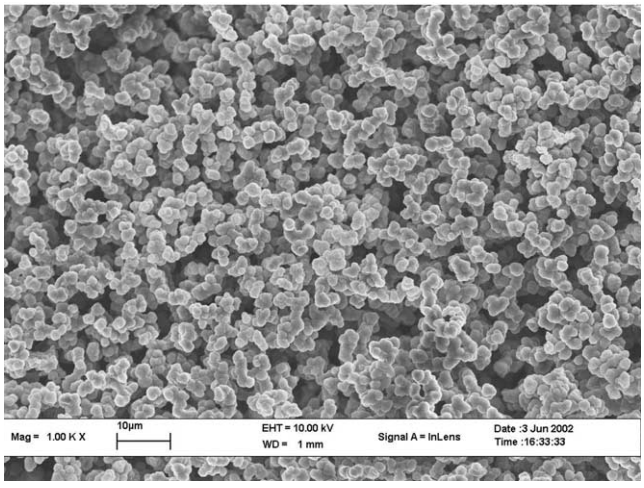

Fig. 4. SEM images of samples by hydro-pressing (upper) and gel-casting (lower).

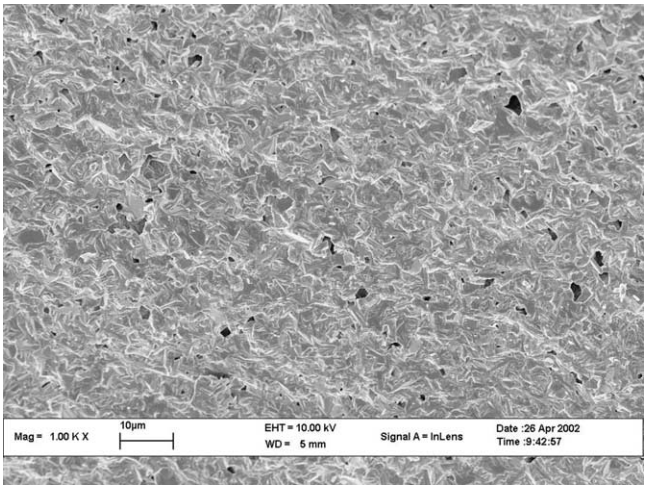

Fig. 5. SEM of ceramic hydro-pressed and sintered at high speed of heating (600 °C h^{-1}).

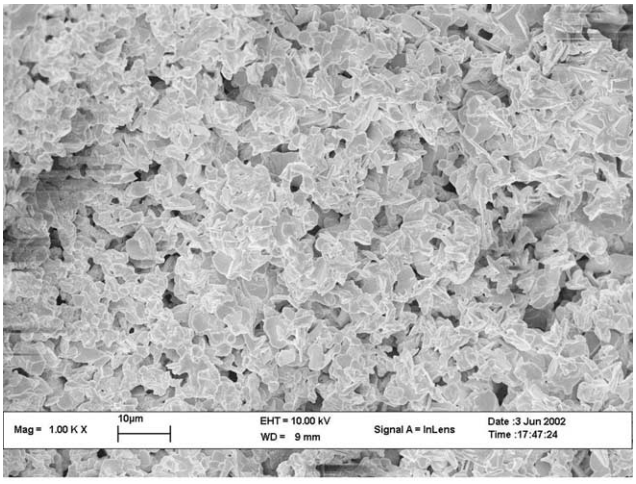

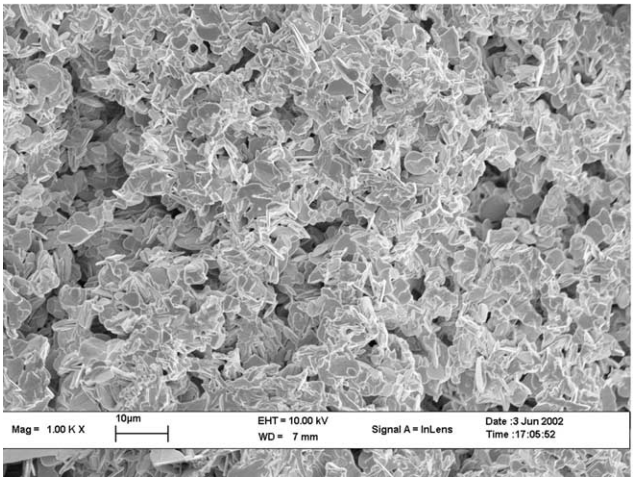

Fig. 6. Microstructure of ceramics sintered at 60 °C h^{-1} (upper), and, at 600 °C h^{-1} (lower).

Meanwhile, different heating speeds of sintering were applied for the green bodies by gel-casting (Fig. 6). It seems that there were less and smaller pores within the ceramics sintered at low heating speed, due to time-consuming of binder removal.

3.4. Hysteresis loops of the ceramics

The hysteresis loops of ceramics with $x = 0.05$ sintered at 1220 °C and $x = 0.4$ obtained at 1260 °C for 90 min were displayed in Fig. 7, upper and lower, respectively. Quantitative data involved $P_{max} = 0.645$ μC cm^{-2}, $P_r = 0.15$ μC cm^{-2} and $V_c = 417$ V, and, $P_{max} = 0.264$ μC cm^{-2}, $P_r = 0.124$ μC cm^{-2} and $V_c = 1102$ V, respectively. It seems that such kind of ceramics behave a weak ferroelectricity.

3.5. Dielectric properties of the ceramics

The temperature dependence of dielectric constant and quality factor of ceramics with $x = 0.2$ and 0.3 were

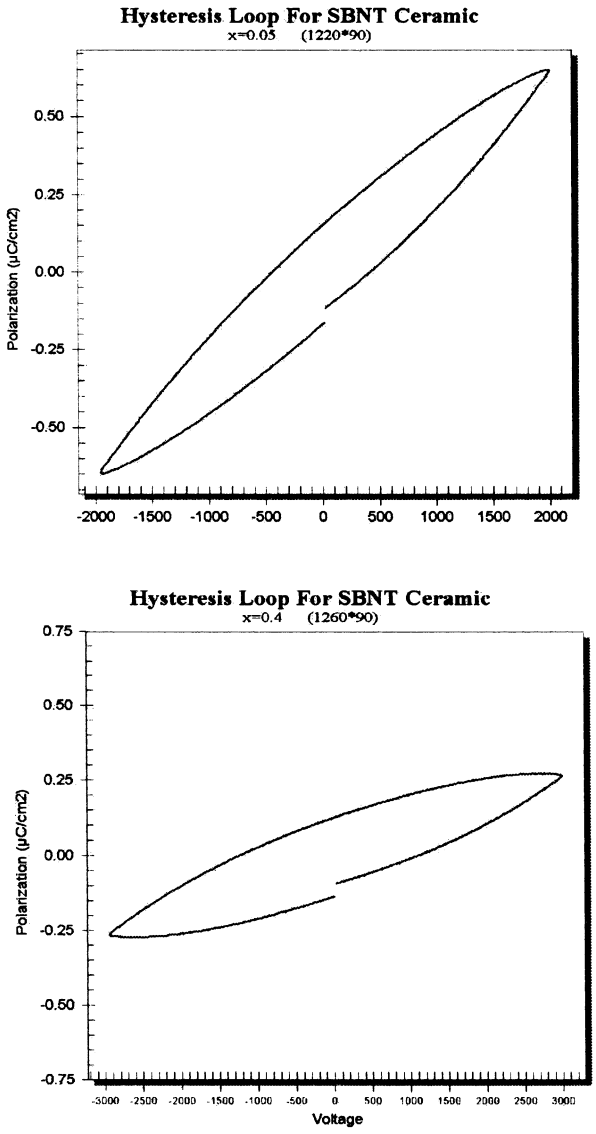

Fig. 7. Hysteresis loops of the ceramics with $x = 0.05$ (upper) and $x = 0.4$ (lower).

measured at $f = 1$ kHz (Fig. 8). It can be seen that the dielectric constant of ceramics are quite stable, while the quality factor of ceramics vary somewhat with temperature.

The dielectric properties of ceramics were moreover dependent on the frequency, as shown in Fig. 9. With increasing of frequency, dielectric constant of the ceramics was decreased, while quality factor was enhanced in the range of lower frequency.

Dielectric properties of ceramics prepared with different x value and sintering condition were measured at $f = 10$ GHz, as shown in Table 1. It can be seen that dielectric constants of the ceramics equal to 80–110 for different compositions and sintering conditions. The quality factors, meanwhile, vary from 135 to 2034 GHz. In addition, best sintering temperature (T_s) for different composition was obtained as following,

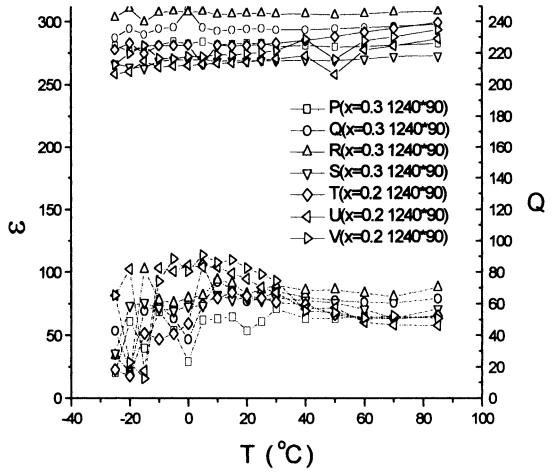

Fig. 8. Temperature dependence of dielectric properties of the ceramics.

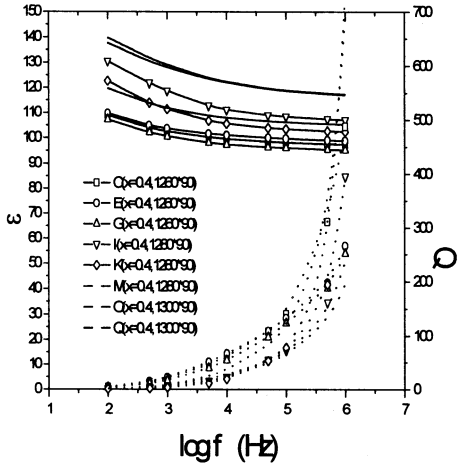

Fig. 9. Frequency dependence of dielectric properties of ceramics.

x value	T_s (°C)
0.05	1180
0.1	1220
0.2	1220
0.3	1240
0.4	1260
0.5	1280

4. Conclusion

$Sr(Bi_{1-x}Nd_x)_8Ti_7O_{27}$ ceramics for wireless technologies were prepared by a solid-state reaction route, shaped by hydro-pressing or gel-casting. Dielectric properties of the samples were measured, displaying

Table 1
Data for ceramics with different x value and sintering condition

Sample No.	x value ($T \times t$)	Diameter (mm)	Thickness (mm)	Dielectric constant	Qf (GHz)
1	0.05 (1180 × 90)	12.36	3.26	87	193
2	0.05 (1200 × 90)	12.23	4.76	81	130
3	0.05 (1220 × 90)	12.78	3.32	79	119
4	0.1 (1200 × 90)	12.72	4.78	99	526
5	0.1 (1220 × 90)	12.7	3.3	97	745
6	0.1 (1240 × 90)	12.8	3.3	86	142
7	0.2 (1220 × 90)	12.84	3.26	100	436
8	0.2 (1240 × 90)	12.82	3.18	103	225
9	0.2 (1260 × 90)	12.8	3.28	101	305
10	0.3 (1220 × 90)	12.76	4.58	101	188
11	0.3 (1240 × 90)	12.7	4.68	104	358
12	0.3 (1260 × 90)	12.7	3.24	89	135
13	0.4 (1260 × 90)	12.74	3.24	95	751
14	0.4 (1280 × 90)	12.6	4.58	108	2034
15	0.4 (1300 × 90)	12.5	4.7	101	738
16	0.5 (1260 × 90)	12.66	4.8	89	243
17	0.5 (1280 × 90)	12.82	3.24	98	876
18	0.5 (1300 × 90)	12.6	3.2	99	321

dielectric constant $\varepsilon = 80$–110 and $Qf = 120$–2100 GHz at 10 GHz.

References

[1] W. Wersing, Electronic Ceramics, Elsevier Applied Science, London, 1991.
[2] D.J. Masse, R.A. Readey, C.P. Hartwig, IEEE 59 (1971) 1628.
[3] J.K. Plourde, D.F. Linn, J. Am. Ceram. Soc. 58 (1975) 418.
[4] D. Hennings, P. Schnabel, Philips J. Res. 38 (1983) 295.
[5] F. Galasso, J. Pyle, Inorg. Chem. 2 (1963) 482.
[6] S. Nomura, Ferroelectrics 49 (1983) 61.
[7] H.M. O'Bryan, Jr., J. Thomson, Jr., J. Am. Ceram. Soc. 57 (1974) 522.
[8] T. Negas, G. Yeager, S. Bell, N. Coats, I. Minis, Am. Ceram. Soc. Bull. 72 (1993) 80.
[9] P.K. Dutta, J.R. Gregg, Chem. Mater. 4 (1992) 843.
[10] R. Gilissen, Mater. Des. 68 (2000) 251.
[11] E.H. Ni, Rev. Sci. Instrum. 68 (1997) 2524.